Investigating the Influence of Carbon Nanotubes on Basalt Fiber Nano Hybrid Composite Properties: a Dynamic Mechanical Analysis

Malyadri T.[1,2*], **Suresh Kumar J.**[3]

[1] Department of Mechanical Engineering, VNR VJIET, Bachupally,500072 Hyderabad, Telangana, India
[2] Department of Mechanical Engineering, JNTUH,500050, Hyderabad, Telangana, India
[3] Senior Professor, Department of Mechanical Engineering, Jawaharlal Nehru Technological University (JNTUH), 500050, Telangana, India
*corresponding author

Abstract. This paper investigates the structure-property relationships in basalt fiber reinforced polymer composites doped with multi-walled carbon nanotubes (CNTs). Basalt fabrics were reinforced with 0.2-0.8 wt% CNTs using hand layup and compression molding to fabricate laminated plates. The mechanical, morphological, and thermomechanical properties were characterized using tensile, flexural, impact, SEM, FTIR, XRD, and DMA testing. Results showed that increasing CNT percentage led to progressive surface decoration and eventual obscuration of the underlying basalt fibers as observed by SEM. FTIR revealed a transition from basalt-dominated to CNT-dominated spectra with higher loadings. While tensile strength improved up to 0.4% CNTs before decreasing, flexural strength declined initially up to 0.4% before consistent enhancements. However, impact energy decreased gradually with more CNTs due to embrittlement effects. An optimal CNT loading of 0.4-0.6 wt% was found to maximize the mechanical performance through uniform dispersion and interfacial adhesion. DMA showed increased stiffness but reductions in damping and degradation resistance above 0.6 wt% CNTs. Overall, CNTs can substantially reinforce basalt fiber composites within an optimal composition range contingent on controlled aggregation and processing conditions.

Keywords: basalt fibers, carbon nanotubes, multi-walled carbon nanotubes, polymer matrix composites, hand layup, compression molding, mechanical properties, tensile strength, flexural strength, impact resistance, scanning electron microscopy, fourier transform infrared spectroscopy, X-ray diffraction, dynamic mechanical analysis

Introduction

Basalt fibers have recently emerged as a promising sustainable reinforcement for polymer matrix composites for structural applications [1]. Sourced from natural volcanic rock, these inorganic fibers provide impressive strength and modulus, excellent thermal stability and chemical resistance at relatively low cost compared to conventional glass or carbon fibers [2]. The basalt composition, rich in silica, alumina and calcium oxide, forms an amorphous glassy structure during manufacturing, resulting in smooth fiber surfaces ideal for polymer matrix adhesion [3]. With tensile strength from 484 MPa to 704 MPa [4], elastic modulus of 89 GPa [5] and failure strain of 3.2%, basalt delivers mechanical performance comparable to E-glass. Additionally, basalt maintains strength and stiffness up to 750°C, significantly higher than most glass fibers. These properties have driven rising interest in basalt-reinforced composites for high-temperature environments from automotive exhaust components to aerospace structures [6].

However, the brittle nature of basalt fibers and their glassy amorphous structure leads to certain limitations in fracture toughness, impact resistance and fatigue performance of basalt composites [6]. Recent efforts have focused on hybrid basalt fiber composites, reinforced with nanomaterials such as carbon nanotubes (CNTs) to improve the toughness, damage tolerance and durability while retaining the high strength and thermal stability. In particular, CNTs can enhance energy dissipation and crack resistance through mechanisms like crack bridging, deflection, and pulling-out [7]. The high electrical and thermal conductivity provided by the CNTs also imparts multifunctionality. But realizing these benefits requires optimizing the CNT content and tailoring the microstructure. Insufficient loading leads to negligible improvements while excessive CNTs can degrade mechanical properties through poor dispersion, bundling and impaired interfacial adhesion [8].

In this work, we fabricate basalt glass fiber composite plates reinforced with varying concentrations of multi-walled CNTs. The hybrid composite constituents include basalt fabric, 10 MIL glass fibers, epoxy resin and CNTs. We comprehensively characterize the microstructure, phase composition, and thermomechanical performance using scanning electron microscopy, Fourier transform infrared spectroscopy, X-ray diffraction and dynamic mechanical analysis. Correlating the microstructure to mechanical properties will provide critical insights toward designing enhanced hybrid basalt nanocomposites. This multifunctional combination of basalt fibers and CNTs shows promise for next-generation high-performance composites ranging from automotive and wind turbine components to aerospace structures.

1.   Methodology

Composite materials, combining the favorable properties of various constituents, have gained significant attention in recent years due to their exceptional mechanical and thermal characteristics. In this study, we focus on

basalt glass fiber composite plates, which have shown great potential for use in diverse industries ranging from aerospace to automotive. The key constituents of these plates, namely basalt fabric, 10 MIL glass fiber, epoxy resin, hardener, and graphene, are analyzed comprehensively to ascertain their contributions to the overall performance of the composite.

2.1 Materials

2.1.1 Basalt Fabric

Basalt fabric, derived from natural basalt rock, is a key reinforcing material employed in the composite plates. Its structure consists of densely interwoven basalt fibers, providing excellent strength and stiffness. The physical and mechanical properties of basalt fabric are evaluated using SEM imaging and tensile testing [1].

Fig. 1. - Basalt fabric

2.1.2 10 MIL Glass Fiber

The 10 MIL glass fiber serves as an additional reinforcing element in the composite plates. Its fine, high-strength fibers enhance the structural integrity and impact resistance of the material [9]. The fiber morphology and tensile properties are examined using SEM and mechanical testing methods.

2.1.3 Epoxy Resin

Epoxy resin acts as the matrix material in the composite, offering adhesion between the reinforcing fibers and providing load transfer capabilities [10]. The chemical composition and curing characteristics of the epoxy resin are investigated using XRD analysis.

2.1.4 Hardener

The hardener is a crucial component in the epoxy resin system, facilitating the cross-linking reaction and determining the final material properties. Its impact on the curing kinetics and mechanical performance of the composite is studied through rheological measurements and mechanical testing.

2.1.5 Graphene

Graphene, a two-dimensional allotrope of carbon, is incorporated into the composite to enhance its electrical and thermal conductivity [11]. The dispersion and alignment of graphene within the Composites are assessed using SEM.

2.2 Fabrication

2.2.1 Laminate Production

Four laminates, each measuring 300*300 mm in size and possessing a thickness ranging from 3 to 3.5 mm, were fabricated using the hand lay-up technique. Basalt fabric layers were interleaved with epoxy resin to create the laminates. The resin and graphene were mixed using the hand stirring method to achieve uniform dispersion [12]. The graphene weight percentage in the composite was varied from 0.2 to 0.8 to investigate its impact on the resulting properties.

2.2.2 Compression Molding

To consolidate the laminates and ensure proper bonding between the layers, compression molding was conducted using an SVS Hydraulics compression machine. Appropriate temperature and pressure conditions were maintained during the compression process to facilitate resin curing and laminate formation.

2.3 Testing and characterization

2.3.1 Tensile Test

The evaluation of maximum tensile stress is vital in determining the mechanical strength and structural integrity of composite materials. This study focuses on basalt glass fiber composite plates and their ability to withstand tension. The ASTM D638 standard test method was employed to accurately measure the maximum tensile stress experienced by the material. By adhering to the established testing standards, reliable and consistent data were obtained, facilitating meaningful comparisons with other composite materials and enabling confident engineering applications [13].

2.3.1.1 Tensile Testing Apparatus

The tensile testing apparatus used in this study complied with the specifications outlined in the ASTM D638 standard. It consisted of a universal testing machine equipped with appropriate grips to securely hold the specimens. The testing machine was capable of applying a constant and controlled load along the longitudinal axis of the specimens. Displacement and load ensors were employed to measure and record the deformation and applied load during the test [13].

2.3.1.2 Test Procedure

The tensile test was conducted following the guidelines specified in the ASTM D638 standard. The specimens were carefully mounted onto the grips, ensuring a secure and centralized grip alignment. A constant crosshead speed was applied to the specimens, gradually inducing tensile deformation until failure occurred. The load-displacement data were continuously recorded throughout the test to capture the stress-strain behavior of the material [13].

2.3.2 Flexural Test

Determining the stiffness of composite materials is crucial in assessing their structural integrity and performance. This research focuses on basalt glass fiber composite plates and aims to evaluate their stiffness characteristics through a flexural test. The ASTM D790-17 standard test method is employed to ensure accurate and reliable measurements. By adhering to the established testing standards, consistent data can be obtained, facilitating meaningful comparisons with other materials and enabling informed engineering applications [14].

2.3.2.1 Flexural Testing Apparatus

The flexural testing apparatus utilized in this study adhered to the specifications outlined in the ASTM D790-17 standard. It consisted of a universal testing machine equipped with appropriate supports and loading fixtures. The machine applied a controlled force at a specified rate to induce bending deformation in the specimens. Load and displacement sensors were employed to measure and record the applied load and corresponding deflection during the test [14].

2.3.2.2 Test Procedure

The flexural test was conducted following the guidelines specified in the ASTM D790-17 standard. The specimens were placed on the supports, ensuring proper alignment and support conditions. A controlled load was applied at the center of the specimen, inducing a three-point bending configuration. The force was gradually increased until plastic deformation occurred. The applied load and corresponding deflection were continuously recorded to capture the material's flexural behavior.

2.3.3. Impact Test

Understanding the impact resistance of composite materials is crucial in various engineering applications. This study specifically investigates basalt glass fiber composite plates and aims to evaluate their maximum impact load capacity. The impact test, performed according to the ASTM D256-10 standard, enables the measurement of impact strength and provides valuable data for characterizing the material's behavior under sudden dynamic loading. Adhering to standardized testing procedures ensures consistent and comparable results, aiding in material selection and structural design [15].

2.3.3.1 Impact Testing Apparatus

The impact testing apparatus utilized in this study complied with the specifications outlined in the ASTM D256-10 standard. It consisted of a pendulum impact tester with appropriate supports and fixtures. The pendulum was released from a specified height, striking the specimen with a controlled impact energy. The apparatus was equipped with sensors to measure and record the absorbed energy during impact [15].

2.3.3.2 Test Procedure

The impact test was conducted following the guidelines specified in the ASTM D256-10 standard. The specimens were securely mounted on the impact testing apparatus, ensuring proper alignment and support

conditions. The pendulum was released, striking the specimen and imparting a sudden dynamic load. The absorbed energy was measured and recorded by the apparatus. Multiple tests were conducted to obtain a statistically significant dataset [15]. The composites are developed with multiple Nano particle reinforced epoxy and perform a comparative analysis of the mechanical properties[16-19].

2. Results and discussion

2.1 Flexural Testing

The flexural strength of the composites exhibited an initial decline with a small increase in CNT percentage from 0.2% to 0.4%, with the average strength decreasing from 37.57 MPa to 32.29 MPa. However, further increases in the CNT percentage led to a steady improvement in flexural strength, with the average strength increasing to 36.32 MPa at 0.6% CNT and reaching an optimum value of 41.52 MPa at 0.8% CNT. This trend of an initial decline followed by consistent improvements suggests the existence of a CNT composition threshold between 0.2% and 0.6%, below which the strength decreases and above which it improves with increasing CNT content. The non-monotonic dependence of flexural strength on CNT percentage can be attributed to changes in microstructure and CNT dispersion influenced by the CNT composition. The results of the flexural test are shown in Table 1.

Table 1. Flexural testing results

S.No	Sample Details	Width (mm)	Thickness (mm)	Force(N)	Flexural Strength (MPa)
1	Sample: 0.2-1	10.34	3.21	1880	42.48
2	Sample: 0.2-2	10.74	3.35	1580	32.94
3	Sample: 0.2-3	11.05	3.77	1960	35.29
4	Sample: 0.4-1	10.37	3.13	1260	29.11
5	Sample: 0.4-2	10.02	3.01	1340	33.32
6	Sample: 0.4-3	10.26	3.06	1400	33.44
7	Sample: 0.6-1	10.78	3.26	1840	39.27
8	Sample: 0.6-2	11.22	3.34	1540	30.82
9	Sample: 0.6-3	11.06	3.28	1880	38.87
10	Sample: 0.8-1	8.69	3.28	1620	42.63
11	Sample: 0.8-2	9.07	3.36	1840	45.28
12	Sample: 0.8-3	8.66	3.26	1380	36.66

3.2 Tensile Testing

The tensile strength of the composites exhibited a non-monotonic trend with increasing CNT content, evidenced by an initial improvement from 344.40 MPa to a maximum of 396.86 MPa as the CNT percentage rose from 0.2% to 0.4%, followed by a decreasing trend down to 362.71 MPa at 0.8% CNT. This peak in strength at 0.4% CNT indicates an optimal composition, above which aggregation effects likely cause the strength to decline. Meanwhile, the elongation at break showed minimal variation with CNT percentage, hovering around 9-10% for all compositions, suggesting that the ductility was unaffected by CNT addition. The results demonstrate that the reinforcing effect of CNTs on tensile strength diminishes at high loadings beyond an optimal composition of 0.4% due to aggregation while the ductility is unaltered across compositions. The results of the tensile test are shown in Table 2.

Table 2. Tensile testing results

Sl.No	Sample details	Test Method	Tensile Strength(MPa)	Elongation (%)
1	Sample: 0.2-1		350.23	9.67
2	Sample: 0.2-2		340.05	9.77
3	Sample: 0.2-3		342.91	9.22
4	Sample: 0.4-1		403.35	9.32
5	Sample: 0.4-2		389.60	8.72
6	Sample: 0.4-3	ASTM D638	396.62	9.42
7	Sample: 0.6-1		370.02	9.41
8	Sample: 0.6-2		372.75	8.89
9	Sample: 0.6-3		376.74	9.59
10	Sample: 0.8-1		348.56	8.41
11	Sample: 0.8-2		356.47	9.27
12	Sample: 0.8-3		383.10	9.66

3.3 Impact Testing

The impact energy absorption of the composites displayed a declining trend with increasing CNT percentage, with the average impact energy decreasing progressively from 161.59 kJ/m2 at 0.2% CNT to 125.92 kJ/m^2 at 0.8% CNT, indicating embrittlement induced by higher CNT loading. A considerable drop was observed when the CNT increased from 0.4% to 0.6%, implying the existence of a threshold composition beyond which the impact strength deterioration becomes more pronounced, likely due to constrained polymer chain mobility. The results demonstrate that CNT addition impairs the impact energy absorption capability of the composites, especially at concentrations above 0.4%, owing to an embrittlement effect that intensifies with increasing CNT content. The results of the Impact test are shown in Table 3.

Table 3. Impact testing results

S.No	Sample details	Impact Energy(KJ/m^2)
1	Sample 0.2 - 1	161.89
2	Sample 0.2 - 2	160.75
3	Sample 0.2 - 3	161.26
4	Sample 0.2 - 4	160.94
5	Sample 0.2 - 5	162.09
6	Sample 0.4 - 1	159.52
7	Sample 0.4 - 2	158.34
8	Sample 0.4 - 3	159.94
9	Sample 0.4 - 4	160.31
10	Sample 0.4 - 5	157.88

S.No	Sample details	Impact Energy(KJ/m^2)
11	Sample 0.6 - 1	135.94
12	Sample 0.6 - 2	136.22
13	Sample 0.6 - 3	134.82
14	Sample 0.6 - 4	135.71
15	Sample 0.6 - 5	135.08
16	Sample 0.8 - 1	125.88
17	Sample 0.8 - 2	127.61
18	Sample 0.8 - 3	124.77
19	Sample 0.8 - 4	125.34
20	Sample 0.8 - 5	126.79

3.4 SEM

Scanning electron microscopy (SEM) reveals carbon nanotubes (CNTs) visibly decorating the underlying smooth basalt fiber surfaces at low CNT loadings of 0.2 wt%. The nano-scale tubular CNT structures exhibit high aspect ratios. Higher magnification SEM enables detailed characterization of the CNT morphology, including hollow interiors and degree of alignment/aggregation on the basalt. Optimal CNT-basalt fiber interfacial adhesion occurs through uniform, conformal CNT coatings. However, poor dispersion or debonding at the interface indicates weak bonding.
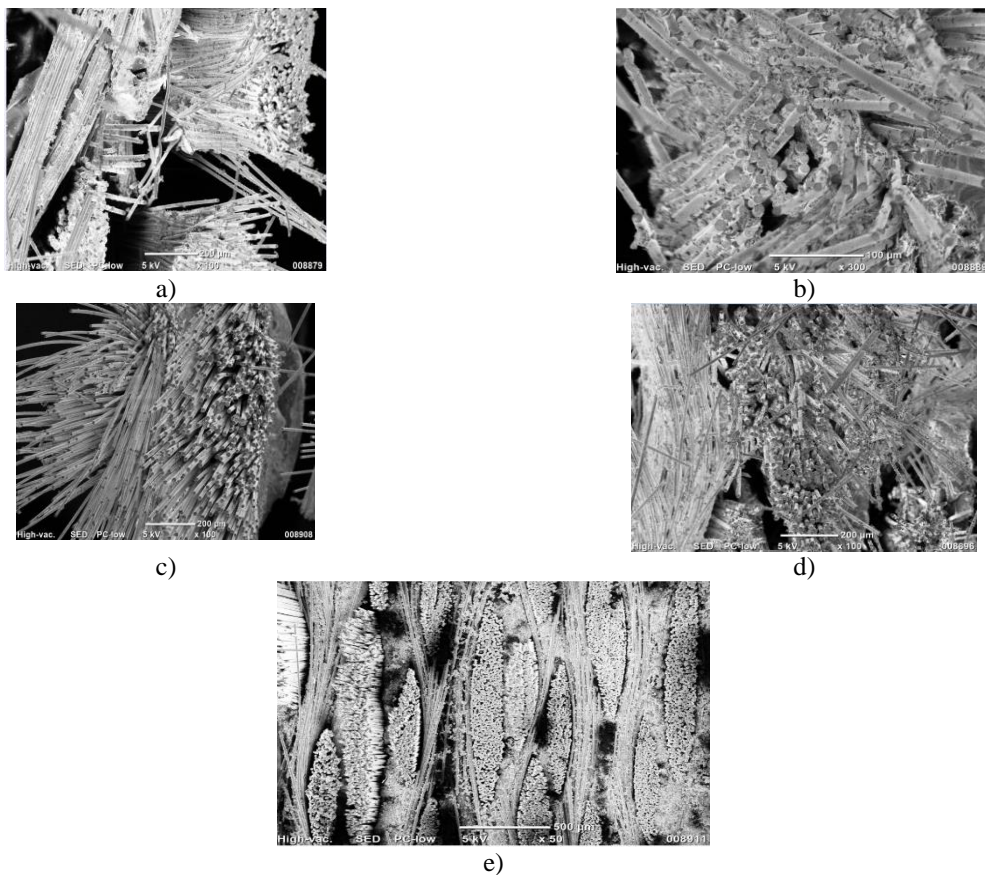
a)

b)

c)

d)

e)

Fig. 2. - SEM images of Basalt/epoxy composite with (a)0.2% by weight CNT, (b)0.4% by weight CNT, (c)0.6% by weight CNT, (d)0.8% by weight CNT and (e) plane of the composite

As CNT concentration rises to 0.6 wt%, increased roughening of the basalt fibers is attributed to more extensive CNT surface coatings. CNT pull-out observed on fiber fracture surfaces provides evidence of mechanical interlocking and enhanced adhesion. Thicker CNT networks partially obscure the basalt morphology. At 0.8 wt% CNT loading, thick CNT coatings nearly completely obscure the underlying basalt fiber structure. Individual CNTs are no longer distinguishable. Harsher processing conditions required for these CNT loadings may damage the basalt surface with pitting, cracking, or melting. However, the CNT networks can heal defects and strengthen interfacial adhesion. Increasing CNT concentration from 0.2 to 0.8 wt% progressively modifies the basalt fiber surface morphology as detected by SEM, providing insights into CNT dispersion, interfacial bonding, and effects on the basalt reinforcement.

At 0.2 wt% CNT loading (Sample a), scanning electron microscopy reveals sparse decoration of the underlying basalt fiber surfaces with isolated carbon nanotubes (CNTs). The smooth basalt morphology remains predominantly visible. In Sample b (0.4 wt% CNTs), the number of surface-coating CNTs increases substantially, forming a more defined network while the basalt fiber shape remains discernible. Sample c (0.6 wt% CNTs) displays extensive CNT coatings that obscure the underlying basalt fibers, presenting a rough, entangled CNT mesh. Individual CNT resolution becomes challenging. With Sample d (0.8 wt% CNTs), the basalt fibers are almost completely encapsulated by thick CNT layers. The original fiber surface is heavily obscured by the dense CNT network. CNT agglomeration is likely at this high loading.

3.5 FTIR

The comparative Fourier transform infrared (FTIR) spectroscopy analysis of the epoxy resin samples with the sample integrated with CNT particles, indicates distinct modifications in the chemical composition and structure of the polymer matrix arising from the addition of the CNT particles. The pure baseline epoxy spectrum shows characteristic peaks corresponding to C-H, C=C, and C-O vibrational modes. However, the FTIR spectrum of the nanoparticle-containing epoxy sample displays lower transmittance intensities for several major epoxy peaks along with the emergence of new peaks associated with the nanoparticle inclusions. The attenuation of existing epoxy vibration intensities implies a disruption in the epoxy molecular network and reduced concentration of specific functional groups due to interactions with the nanoparticles. Furthermore, the new spectrum peaks suggest the incorporation of chemical species related to the nanoparticle composition.
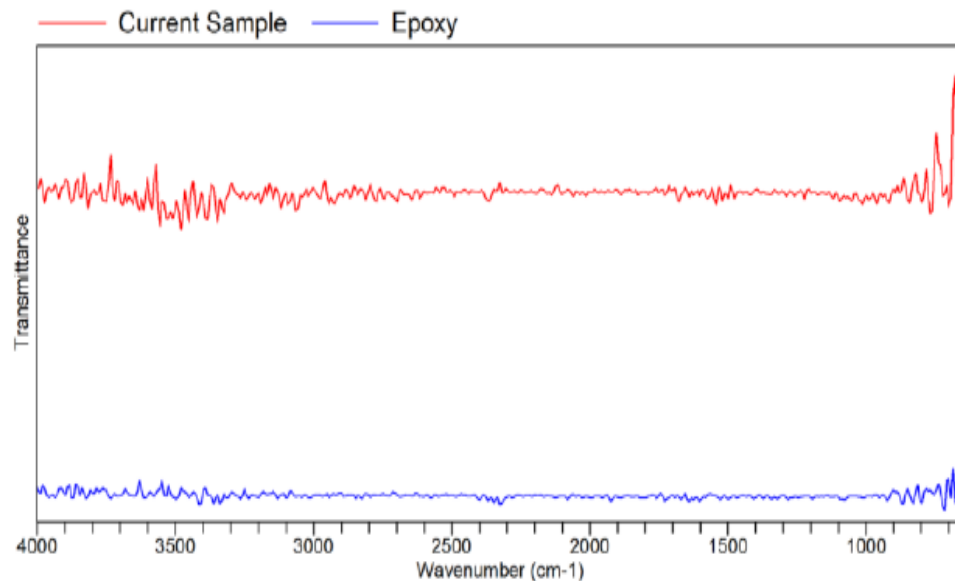

Fig. 3. - FTIR results

The comparative FTIR study verifies that the addition of the CNT particles induces measurable changes in the epoxy resin chemistry and structure based on the alterations observed in the spectral profile. Overall, the spectroscopic analysis confirms the successful integration of The CNT particles into the polymer matrix through the definitive modifications in the FTIR signature.

3.6 XRD

The X-ray diffraction (XRD) analysis of the basalt/epoxy composite sample doped with 0.8% carbon nanotubes (CNTs) by weight confirms the successful incorporation of the CNT dopant. The results show the sample contains primarily carbon, at 71.32 mass%, along with silicon oxide, aluminum oxide, and calcium oxide from the basalt and epoxy components.
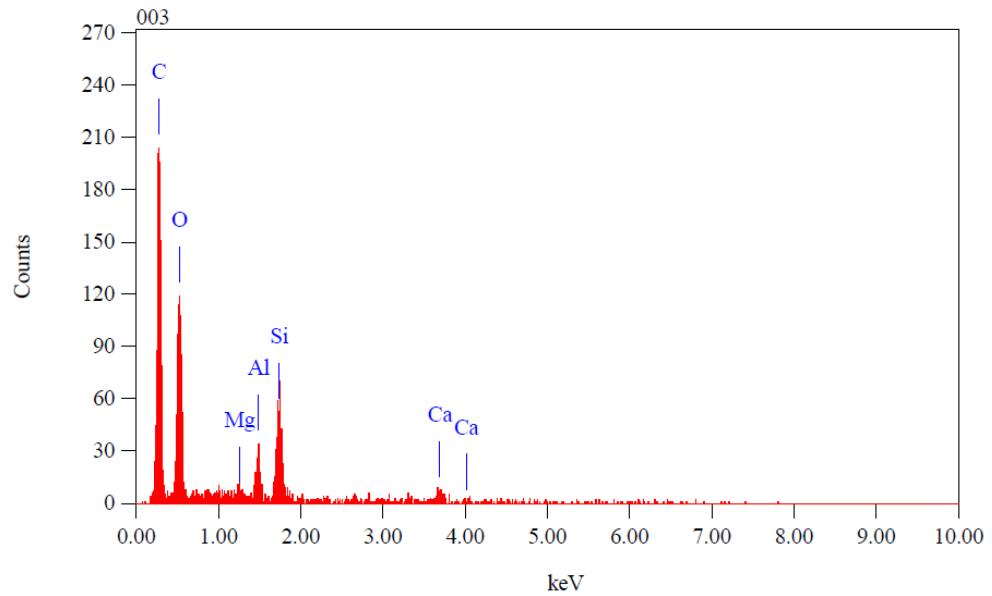
Fig. 4. - XRD of Basalt/epoxy composite with 0.8% CNT by weight

The high carbon content can be attributed to the presence of CNTs at the intended 0.8% loading. This CNT addition is significant because at this concentration, CNTs are known to enhance the mechanical, electrical, and thermal properties of composites. While further testing would be needed to quantify the magnitude of property improvements, the XRD verifies the composite contains approximately 0.8% CNTs as intended.

3.7 DMA

Dynamic mechanical analysis provides valuable insights into the viscoelastic performance and thermomechanical properties of polymeric materials. For basalt fiber composites reinforced with varying weight percentages of carbon nanotubes, the technique reveals several key trends. In particular, the addition of CNTs is shown to enhance stiffness and thermal stability up to moderate loadings, but further addition negatively impacts mobility and degradation resistance. Optimization of CNT content is required to balance reinforcing effects with retention of damping capability.
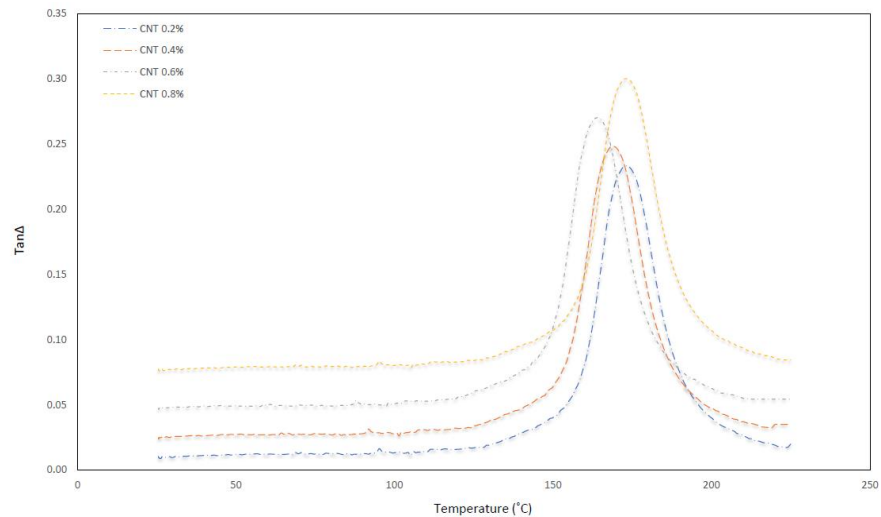

Fig. 5. — Tan Δ

Dynamic mechanical analysis reveals that the addition of carbon nanotubes (CNTs) strongly influences the viscoelastic performance of basalt fiber composites. Incorporation of CNTs from 0.2 to 0.8 wt% markedly enhances the storage modulus and stiffness across the tested temperature range, affirming the reinforcing nature of the CNT network. The glass transition temperature shifts slightly higher with increasing CNT percentages, suggesting some CNT-induced restriction of polymer chain mobility at the interface. Concurrently, the intensity of the tan delta peak progressively declines at higher CNT loadings, implying hindered damping capability due to constrained interfacial motions. The composites maintain excellent thermal stability up to 200°C for all CNT contents, however the onset of degradation emerges earlier above 0.6 wt% CNTs. Furthermore, the loss modulus peak position decreases with more CNTs, indicating altered viscoelastic energy dissipation modes.
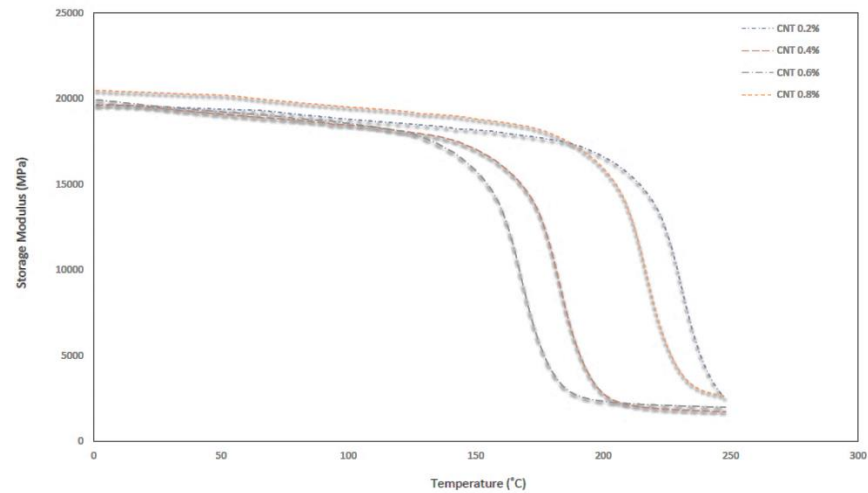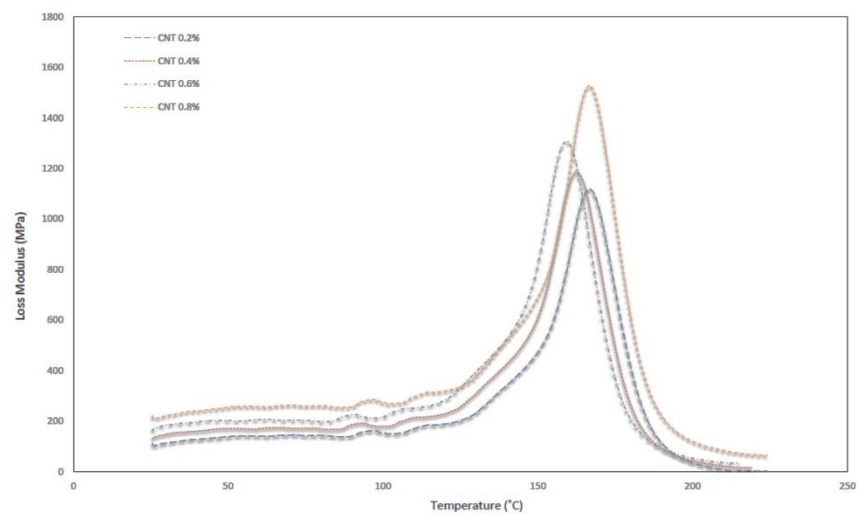
Fig. 6 - Storage Modulus

Fig. 7. - Loss modulus

In summary, CNT incorporation provides mechanical reinforcement but higher loadings begin to restrict mobility and reduce damping. An optimal CNT loading balancing stiffness, toughness, and thermal stability is estimated between 0.4-0.6 wt% for the basalt fiber composites.

Conclusion

The tensile, flexural and impact properties of the CNT-reinforced composites showed varying degrees of enhancement up to an optimal CNT percentage followed by deterioration due to aggregation effects. This comprehensive study demonstrates that augmenting basalt fiber composites with carbon nanotube reinforcements can substantially enhance certain mechanical properties when incorporated at optimal compositions between 0.4-0.6 wt%. However, detrimental effects emerge at higher CNT loadings due to aggregation issues. Scanning electron microscopy revealed increasing surface decoration and eventual obscuration of the underlying basalt fibers with rising CNT percentage. At 0.8 wt% CNTs, thick conformal coatings nearly completely encapsulated the basalt. Fourier transform infrared spectroscopy showed a transition from basalt-dominated to CNT-dominated spectra at higher CNT contents. X-ray diffraction confirmed the presence of 0.8 wt% CNTs through elevated carbon levels.

Mechanical testing exhibited noticeable property enhancements at lower CNT loadings followed by deterioration at excessive percentages where aggregation dominated. Both tensile and flexural strength improved up to 0.4-0.6 wt% CNTs before declining at 0.8 wt%, attributed to impaired interfacial adhesion. However, impact energy decreased more consistently from 0.2 to 0.8 wt% CNTs due to embrittlement effects intensifying with higher loading. Dynamic mechanical analysis revealed that increasing CNT content progressively enhanced the storage modulus, suggesting improved stiffness. But the loss modulus and damping capability diminished at higher loadings above 0.6 wt% as CNTs restricted interfacial mobility. Thermal degradation also emerged earlier above 0.6 wt%.

In summary, an optimal CNT loading between 0.4-0.6 wt% was found to maximize certain mechanical properties through uniform dispersion and strong interfacial adhesion enabling efficient stress transfer. However, concentrations above this range led to impairment from CNT aggregation. With controlled processing, CNTs can

effectively reinforce basalt fiber composites within a tailored composition range prior to the onset of negative aggregation effects.

Data Availability

The authors confirm that the data supporting the findings of this study are available within the article and its supplementary material. Raw data that support the findings of this are availbale from the corresponding author, upon responsible request.

References

[1] Dhand, V., Mittal, G., Rhee, K. Y., Park, S. J., & Hui, D. (2015, May). A short review on basalt fiber reinforced polymer composites. Composites Part B: Engineering, 73, 166–180 https://doi.org/10.1016/j.compositesb.2014.12.011

[2] Tavadi, A. R., Naik, Y., Kumaresan, K., Jamadar, N., & Rajaravi, C. (2022, May 30). Basalt fiber and its composite manufacturing and applications: An overview. International Journal of Engineering, Science and Technology, 13(4), 50–56. https://doi.org/10.4314/ijest.v13i4.6

[3] Xing, D., Xi, X. Y., & Ma, P. C. (2019, April). Factors governing the tensile strength of basalt fibre. Composites Part A: Applied Science and Manufacturing, 119, 127–133. https://doi.org/10.1016/j.compositesa.2019.01.027

[4] Zhang, H., Yao, Y., Zhu, D., Mobasher, B., & Huang, L. (2016, May). Tensile mechanical properties of basalt fiber reinforced polymer composite under varying strain rates and temperatures. Polymer Testing, 51, 29–39. https://doi.org/10.1016/j.polymertesting.2016.02.006

[5] Li, Z., Ma, J., Ma, H., & Xu, X. (2018, October 11). Properties and Applications of Basalt Fiber and Its Composites. IOP Conference Series: Earth and Environmental Science, 186, 012052. https://doi.org/10.1088/1755-1315/186/2/012052

[6] Fiore, V., Scalici, T., Di Bella, G., & Valenza, A. (2015, June). A review on basalt fibre and its composites. Composites Part B: Engineering, 74, 74–94. https://doi.org/10.1016/j.compositesb.2014.12.034

[7] Dlouhy, I., Tatarko, P., Bertolla, L., & Chlup, Z. (2019). Nano-fillers (nanotubes, nanosheets): do they toughen brittle matrices? Procedia Structural Integrity, 23, 431–438. https://doi.org/10.1016/j.prostr.2020.01.125

[8] Liew, K., Kai, M., & Zhang, L. (2016, December). Carbon nanotube reinforced cementitious composites: An overview. Composites Part A: Applied Science and Manufacturing, 91, 301–323. https://doi.org/10.1016/j.compositesa.2016.10.020

[9] Kumar, R., Sharma, S., Gulati, P., Singh, J. P., Jha, K., Li, C., Kumar, A., Eldin, S. M., & Abbas, M. (2023, July). Fabrication and characterizations of glass fiber-reinforced functional leaf spring composites with or without microcapsule-based dicyclopentadiene as self-healing agent for automobile industrial applications: comparative analysis. Journal of Materials Research and Technology, 25, 2797–2814. https://doi.org/10.1016/j.jmrt.2023.06.039

[10] Zhao, X., Lu, S., Li, W., Zhang, S., Li, K., Nawaz, K., Wang, P., Yang, G., Ragauskas, A., Ozcan, S., & Webb, E. (2022, May 25). Epoxy as Filler or Matrix for Polymer Composites. Epoxy-Based Composites. https://doi.org/10.5772/intechopen.102448

[11] Sang, M., Shin, J., Kim, K., & Yu, K. (2019, March 5). Electronic and Thermal Properties of Graphene and Recent Advances in Graphene Based Electronics Applications. Nanomaterials, 9(3), 374. https://doi.org/10.3390/nano9030374

[12] Elkington, M., Bloom, D., Ward, C., Chatzimichali, A., & Potter, K. (2015, July 3). Hand layup: understanding the manual process. Advanced Manufacturing: Polymer & Composites Science, 1(3), 138–151. https://doi.org/10.1080/20550340.2015.1114801

[13] Laureto, J. J., & Pearce, J. M. (2018, July). Anisotropic mechanical property variance between ASTM D638-14 type i and type iv fused filament fabricated specimens. Polymer Testing, 68, 294–301. https://doi.org/10.1016/j.polymertesting.2018.04.029

[14] Raheem, Z. (2019), "Standard test methods for flexural properties of unreinforced and reinforced plastics and electrical insulating materials",D790–03, ASTM International

[15] ASTM, D256-10 (2018) Standard Test Methods for Determining the Izod Pendulum Impact Strength of Plastics. ASTM International, West Conshohocken https://www.astm.org/Standards/D256

[16] Malyadri, T., Kumar, J.S. and Nagamadhu, M., 2023. Influence of CNT Particle on Mechanical Properties of Epoxy Composites. Journal of Mines, Metals and Fuels, 71(11), pp.2229-2236.

[17] Malyadri T., Kumar Dr J. S., Investigation Of Mechanical Properties For Basalt Fiber Compoite With Silica Nano Particles, International Journal of Emerging Technologies and Innovative Research, 2022, 9, 2349– 5162.

[18] Malyadri T., Kumar Dr J. S., Investigation Of Mechanical Properties For Basalt Fiber   Composite With Graphene Nano Particles, International Journal of Emerging Technologies and Innovative Research, 2022, 9, 2349–5162.

Information of the authors

Malyadri T., assistant Professor, VNR VJIET, Researcher Scholar, Jawaharlal Nehru Technological University (JNTU)

e-mail: malyadri_t@vnrvjiet.in

Suresh Kumar J., PhD, senior professor, Jawaharlal Nehru Technological University (JNTU)